

Nonlinearity Estimation in Power Amplifiers Based on Subsampled Temporal Data

Jesús Ibáñez-Díaz, Carlos Pantaleón, *Member, IEEE*, Ignacio Santamaría, *Associate Member, IEEE*, Tomás Fernández, and David Martínez

Abstract—In this paper we apply subsampling techniques to capture the temporal input–output relationship of RF power amplifiers. This approach avoids the distortion introduced by the upconverter and downconverter stages. We develop polynomial models with memory from the available data and evaluate their performance by estimating device parameters like adjacent channel power ratio (ACPR) and AM–AM curves. The estimated parameters show good agreement with the empirical ones.

Index Terms—Adjacent channel power ratio (ACPR), AM–AM curve, nonlinear modeling, power amplifier, subsampling.

I. INTRODUCTION

PRECISE and representative power amplifier models are a key factor to simulate an entire communication system and are essential in order to introduce linearization techniques (e.g., predistortion). This work analyzes the distortion caused by power amplifiers driven by wideband signals. The traditional measures (AM–AM and AM–PM curves), characterizations and models (Saleh [1], Poza [2], and Abuelma'atti [3]), which are based on single-tone amplitude sweeps, are not capable of truly representing the device behavior in the context of modern wideband digital modulations (OFDM, CDMA, QAM, ...) with non-constant envelope.

In addition, analog-to-digital (A/D) converters have seen significant advances both in performance and speed, while prices have declined. Advances in digital signal processing are evident and the tendency to substitute analog signal processing by their equivalent digital counterpart is widespread. However, the well-known Nyquist limit represents a very serious obstacle preventing the application of digital signal processing (DSP) techniques at frequencies higher than a few hundred megahertz.

However, sampling at rates lower than the Nyquist limit, twice the maximum frequency, can still allow for an exact reconstruction of the information content of the analog signal if the signal is bandpass. This is the subsampling (or bandpass sampling) technique [4]–[6] that allows exact reconstruction of the original bandpass signal if the sampling rate is at least two times the bandwidth of the signal. An important practical limitation is that the A/D converter (or the track and hold circuit) must still be able to effectively operate on the highest frequency component in the signal.

Manuscript received May 2, 2000; revised March 16, 2001. This work was supported in part by CYCIT Grant 1FD97-1863-C02-01.

The authors are with the Departamento Ingeniería de Comunicaciones, Universidad de Cantabria, Los Castros, Santander, Spain (e-mail: jesus@gtas.dicom.unican.es).

Publisher Item Identifier S 0018-9456(01)06016-8.

Subsampling is a common technique used in several applications, for example, radio receivers using digitization at the intermediate frequency or, in some cases, even at radio frequency. In this paper, we will use this technique for device characterization and to develop polynomial models with memory from the available data. Several authors have presented polynomial memoryless models [7], tapped-delay-line models [8], Hammerstein models [9], and Volterra models or neural network models [10] using input–output temporal measures in order to identify nonlinear systems.

The paper is organized as follows. In Section II, the data acquisition system using subsampling is described. In Section III, several measurements of power amplifiers are presented. Section IV deals with the polynomial models, and Section V presents the main results. Finally, Section VI provides the conclusion.

II. ACQUISITION SYSTEM

A. Subsampling

Bandpass sampling or subsampling consists of sampling a modulated signal using a sampling frequency below the Nyquist rate to achieve frequency translation via intentional aliasing. An ideal bandpass signal has no frequency components below a certain frequency f_l and above a certain frequency f_h . For this bandpass signal, the minimum requirements to allow for an exact reconstruction are that the sampling rate must be at least two times the bandwidth $f_h - f_l$ of the signal. To ensure that spectrum overlapping does not occur, the sampling frequency f_s must satisfy

$$\frac{2f_h}{k} \leq f_s \leq \frac{2f_l}{k-1} \quad (1)$$

where k is restricted to integer values that satisfy

$$2 \leq k \leq \frac{f_h}{f_h - f_l} \quad (2)$$

and

$$f_h \leq 2f_l. \quad (3)$$

Subsampling reduces drastically the sampling rate (k times), but it has the limitation that the A/D converter must still be able to effectively operate on the highest frequency component of the signal. In addition, stringent requirements on analog bandpass filters may be needed to prevent distortion from noise or out-of-band signals.

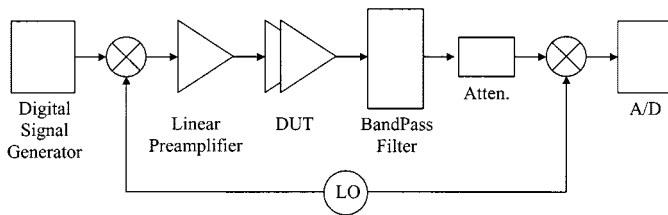


Fig. 1. Traditional measurement scheme.

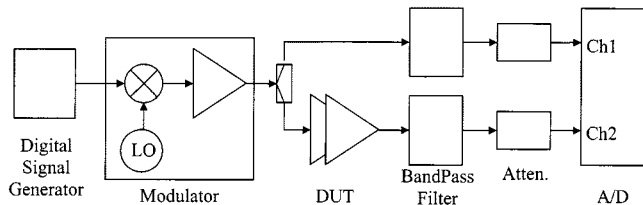


Fig. 2. Proposed measurement scheme.

B. Acquisition Schemes

In the last few years, several methods for temporal characterization of power radio frequency (RF) amplifiers have been developed [7], [11]. All of them use an acquisition scheme based on the sampling of the demodulated signal at baseband, as illustrated in the block diagram of Fig. 1. In this set-up, a test signal is digitally generated and upconverted to a suitable microwave frequency. The signal must be kept at a low level in order to prevent unwanted distortion from the upconverter. Due to the low input signal level, it is necessary to add a low distortion amplifier to be able to observe the saturation characteristics of the power amplifier. A bandpass filter centered at the carrier frequency follows the amplifier and an attenuator is used to minimize the downconverter distortion. Finally, the baseband output signal is sampled at the Nyquist rate.

The main drawback of this scheme is the high linearity requirements of the preamplifier and the upconverter and downconverter mixers. In any case, this method is not able to isolate the power amplifier behavior, since it includes the whole RF chain (upconversion–amplification–downconversion). A good solution to remove frequency conversion errors from such measurement system is proposed in [12] by calibrating the converters, although the final setup is quite complex.

As an alternative, we present a measurement scheme based on the subsampling technique (Fig. 2). A digital signal generator generates the test signal, which is upconverted and preamplified in order to drive the RF power amplifier. An exact replica of the input signal, provided by the splitter, is filtered, attenuated (when the signal level is too high) and subsampled by one A/D converter channel. In the same way, the other A/D channel subsamples the device under test (DUT) output signal after the corresponding filter and attenuator.

The HP model 70820A Transition Analyzer is used to subsample the input and output signal of the DUT at a rate up to 20 Ms/s per channel. Its input bandwidth allows the acquisition of signals centered up to 20 GHz with a bandwidth up to 10 MHz.

The main advantage of this measurement scheme is that it characterizes solely the amplifier behavior, due to the acquisi-

tion of the RF input and output signals. Another improvement is the absence of any downconversion stage. On the other hand, it is not necessary to remove the upconverter and preamplifier errors because the real RF power amplifier input signal will be acquired together with the output signal. Finally, this method avoids the problems related with upconversion and downconversion delays and timing errors.

The A/D converter is a critical concern of this subsampling scheme. It must possess sufficient input bandwidth to follow the highest frequency components of the signal (in the carrier frequency band). In the same way, it must provide an adequate sampling rate in order to capture the bandwidth of the bandpass signal. Nowadays, this last aspect is not restrictive because commercial A/D converters reach hundreds of megasamples per second, and even a few gigasamples per second. This performance allows us to study the amplifier behavior with wide bandwidth driving signals, to relax the bandpass filter specifications, and/or to increase the A/D precision through digital signal processing techniques (oversampling of the subsampled signal and subsequent decimation [13]).

III. MEASUREMENTS

The device used in the measurements was a Motorola model MRFC1818 GaAs MESFET Power Amplifier working at 1455 MHz. Several test signals were generated in order to extract the amplifier behavior and to check the effectiveness of the proposed acquisition and characterization scheme.

In our first approach, we used a coarse representation of an orthogonal frequency division multiplexing (OFDM) signal as a test signal, consisting of a flat spectrum around a central frequency of $f_0 = 5$ MHz, with a large number of unit amplitude carriers having independent random phases of uniform distribution. This scheme results in an amplitude envelope signal having a Rayleigh distribution. A data register of 16 000 samples was uploaded to the HP model 33 120A 40 Ms/s signal generator and periodically repeated at rate of

$$f_{rep} = 40 \text{ Ms/s} / 16\,000 \text{ samples} = 2500 \text{ Hz.} \quad (4)$$

The HP model 89431 RF section translated the signal to the 1.455 GHz band and performed the preamplification.

A record of 15 000 samples per channel was acquired for several input power levels (from -20 dBm to $+5$ dBm). As an example, Fig. 3 shows the input and output amplifier power spectrum using a 1 MHz and 0 dBm OFDM type test signal. The spectral regrowth of the power amplifier output is clear, indicating its nonlinear behavior. Fig. 4 represents the envelope amplitude input–output relationship that clearly shows the saturation effect of the power amplifier for high values of the input.

In the same way, Fig. 5 displays the measured input and output envelope amplitude sequences, showing the great significance of the saturation effect in the power amplifier. Moreover, saturation is not the only remarkable aspect when analyzing the temporal measurements. As Fig. 4 shows, the amplifier presents hysteresis, even in the linear region, which suggests some kind of system memory. Fig. 6 shows the relationship between the measured input and output envelope amplitude signals

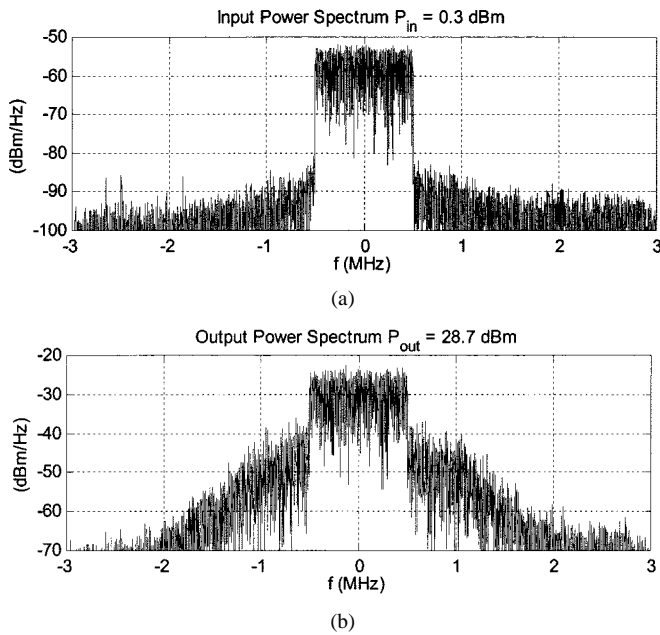


Fig. 3. Measured power spectrum of an OFDM type signal (BW = 1 MHz, $P_{in} = 0$ dBm). (a) Input; (b) output.

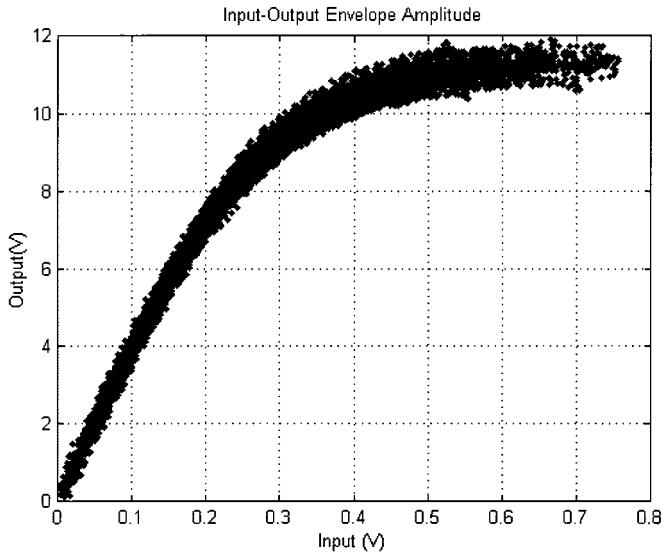


Fig. 4. Measured input-output envelope amplitude of an OFDM type signal (BW = 1 MHz, $P_{in} = 0$ dBm).

of the amplifier fed with a narrowband DSB-AM signal. The modulating signal is a low frequency (20 kHz) sinusoid, and the modulation index is 0.7. For this input signal, the hysteresis is quite evident.

IV. MODELS

Using the available temporal data measurements, we estimated a quadrature nonlinear model similar to the one presented in [14]. A block diagram of the proposed model is shown in Fig. 7.

The in-phase S_I and quadrature S_Q subsystems adjust the output in-phase and quadrature components as a function of the

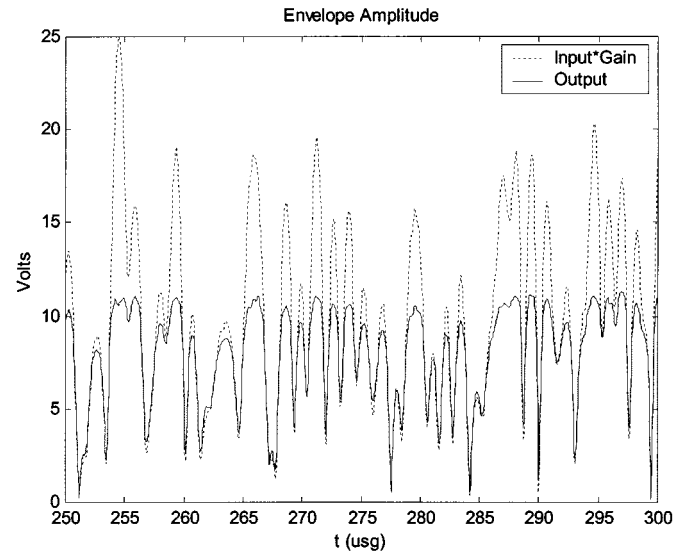


Fig. 5. Measured input and output envelope amplitude signals of an OFDM style signal (BW = 1 MHz, $P_{in} = 0$ dBm).

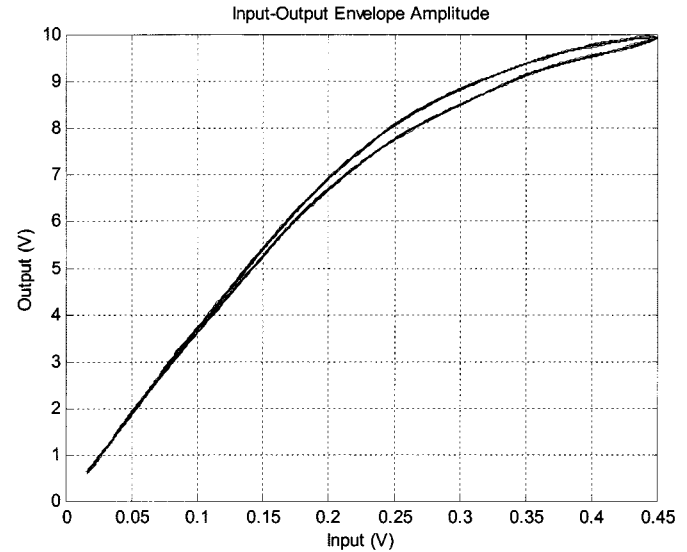


Fig. 6. Measured input-output envelope amplitude of an AM signal.

input envelope amplitude. The in-phase and quadrature models have the following input-output relationship

$$\begin{aligned}\tilde{y}_I[n] &= \sum_{k=0}^{L_I} \sum_{j=1}^{N_I} b_{kj}^I |\tilde{x}[n - kn_0]|^j \\ \tilde{y}_Q[n] &= \sum_{k=0}^{L_Q} \sum_{j=1}^{N_Q} b_{kj}^Q |\tilde{x}[n - kn_0]|^j\end{aligned}\quad (5)$$

where

- L_I and L_Q memory;
- N_I and N_Q highest polynomial order;
- n_0 distance between the memory taps.

Using the amplifier input and output signals, the optimum values of b_{kj}^I and b_{kj}^Q are easily calculated by least squares.

An important advantage of this model is its flexibility, since it can represent the simplest AM-AM model, forcing $L_I = 0$ and $N_Q = 0$, a polynomial memoryless model, with $L_I =$

TABLE I
 SNR_A (dB) USING THE AM ACQUISITION MODEL

N	1	2	3	4	5	6	7	8	9	10
L=0	16.3	34.9	35.3	37.2	37.2	37.3	37.3	37.4	37.4	37.4
L=1, n₀=100	16.5	38.1	40.6	47.1	47.3	48.4	48.7	49.1	49.0	48.9

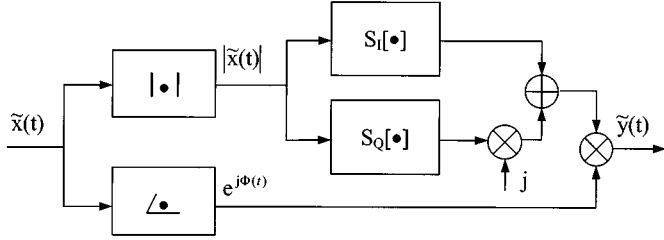


Fig. 7. Quadrature nonlinear model.

$L_Q = 0$, or a more general model with $L_I = L_Q = L$ and $N_I = N_Q = N$.

V. RESULTS

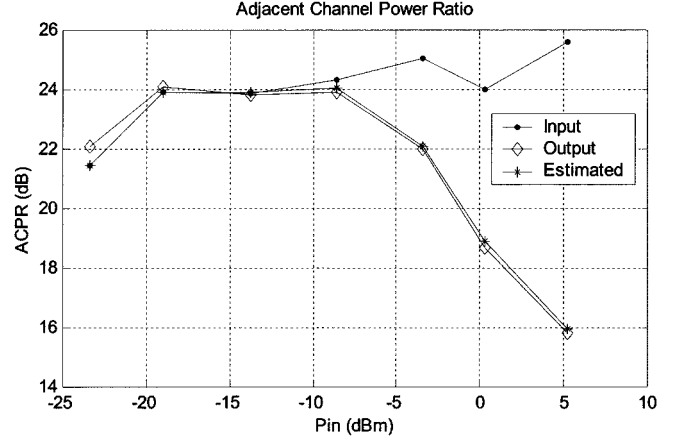
In this section, we construct the models of Section IV from the amplifier measurements obtained in Section III. Then we simulate some amplifier parameters and compare them with those obtained directly from making measurements.

In order to obtain the amplifier model, the first 2000 samples of the temporal acquisitions were used. The rest of the samples (13 000) were used to determine the model accuracy. If we define the estimation error as the mean squared error of the difference between the estimated signal $\hat{y}(t)$ and the measured signal $\tilde{y}(t)$ then the amplitude estimation error \hat{e}_A the in-phase estimation error \hat{e}_I and the quadrature estimation error \hat{e}_Q can be written as

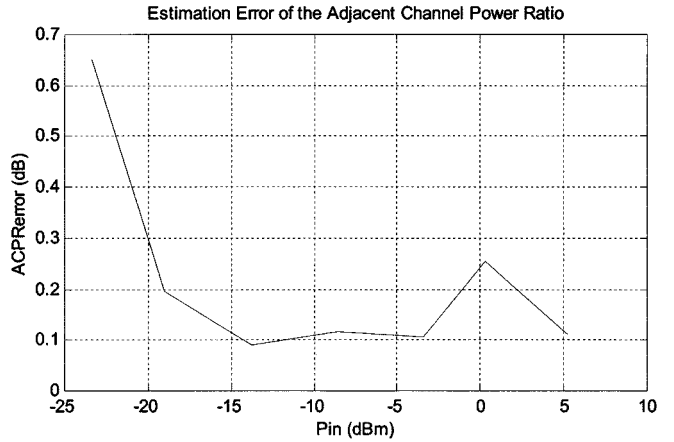
$$\begin{aligned} \hat{e}_A &= \frac{1}{N} \sum_{n=1}^N (|\tilde{y}[n]| - |\hat{y}[n]|)^2 \\ \hat{e}_I &= \frac{1}{N} \sum_{n=1}^N (\text{Re}\{\tilde{y}[n]\} - \text{Re}\{\hat{y}[n]\})^2 \\ \hat{e}_Q &= \frac{1}{N} \sum_{n=1}^N (\text{Im}\{\tilde{y}[n]\} - \text{Im}\{\hat{y}[n]\})^2. \end{aligned} \quad (6)$$

The estimation signal to noise ratios are thus

$$\begin{aligned} \text{SNR}_A &= \frac{1}{N \cdot \hat{e}_A} \sum_{n=1}^N |\tilde{y}[n]|^2 \\ \text{SNR}_I &= \frac{1}{N \cdot \hat{e}_I} \sum_{n=1}^N \text{Re}\{\tilde{y}[n]\}^2 \\ \text{SNR}_Q &= \frac{1}{N \cdot \hat{e}_Q} \sum_{n=1}^N \text{Im}\{\tilde{y}[n]\}^2. \end{aligned} \quad (7)$$



(a)



(b)

Fig. 8. Adjacent channel power ratio (ACPR). (a) Input, output, and estimated ACPR; (b) estimation error of the ACPR.

The MRFC1818 amplifier temporal measurements suggest some kind of memory, which is particularly clear when the amplifier is driven by an AM signal. Table I shows the signal-to-noise ratio (SNR) obtained with different model parameters.

Table I clearly shows the superior performance of the one-tap memory models over the memoryless ones. For example, there is an improvement of 10 dB between the fourth order one-tap model ($\text{SNR}_A = 47.1$, $\text{SNR}_I = 45.2$, $\text{SNR}_Q = 45.3$) and the memoryless fourth order model ($\text{SNR}_A = 37.2$, $\text{SNR}_I = 37.1$, $\text{SNR}_Q = 36.8$).

In order to validate the characterization method based on subsampling, we simulate the adjacent channel power ratio (ACPR) using an amplifier model with $N = 10$ and $L = 1$, and an OFDM style input signal of 1 MHz bandwidth and power in the -20 dBm to 10 dBm range. Fig. 8 compares the simulation results with the measurements. It shows the measured ACPR at the amplifier input and output and the simulated ACPR. The differ-

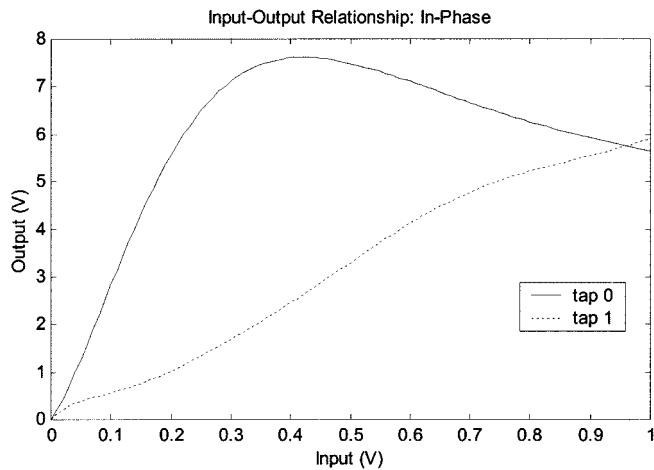


Fig. 9. Amplitude response of the in-phase subsystem model.

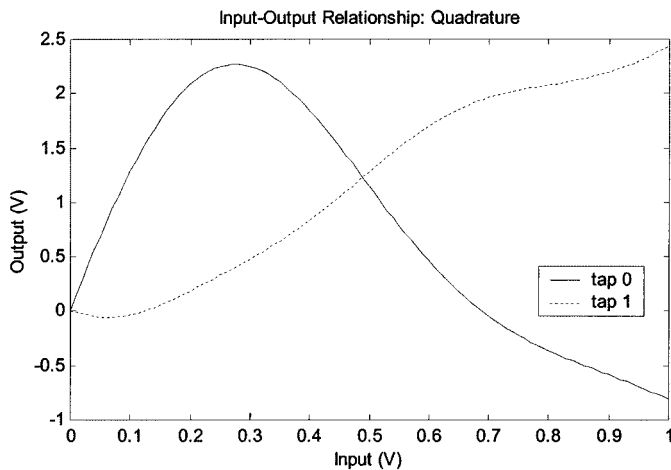


Fig. 10. Amplitude response of the quadrature subsystem model.

ence between the simulated and measured output ACPR is also displayed, showing the great accuracy of the model.

Figs. 9 and 10 show the amplitude response of the in-phase and quadrature subsystems of the two-tap model. The overall amplitude response of the model, driven with a constant envelope input signal, is presented in Fig. 11 and compared with the AM-AM curve measured with the traditional CW methods. Again, a very good agreement is obtained.

VI. CONCLUSION

In this paper, we have successfully applied subsampling techniques to the characterization of RF power amplifiers. This approach allows for solely characterizing the amplifier behavior, avoids the upconverter and preamplifier linearity restrictions, eliminates the downconverter and its distortion, and easily shows the main amplifier characteristics (saturation, hysteresis, and memory). The polynomial memory models developed from the acquired data provide for obtaining amplifier parameters like ACPR and AM-AM curves that show good agreement with empirical measurements. These results validate our subsampling approach.

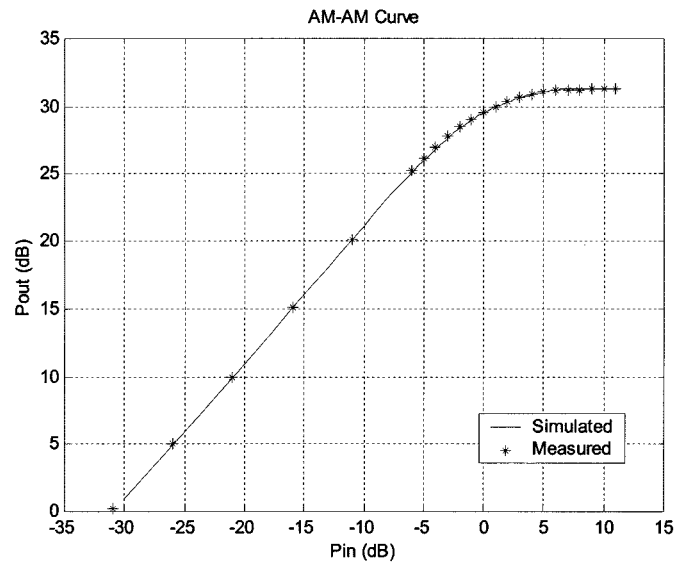


Fig. 11. Simulated and measured AM-AM curve.

Further work is being carried out in order to improve the acquisition scheme. We are using a higher sampling frequency A/D converter that will increase the signal bandwidth and/or the measurement accuracy (decimation). The A/D converter characterization itself is another aspect that will be considered in order to establish its influence on the measurements. Furthermore, this work will allow the development of novel amplifier models and their application to linearization schemes.

REFERENCES

- [1] A. A. M. Saleh, "Frequency-independent and frequency-dependent nonlinear models of TWT amplifiers," *IEEE Trans. Comm.*, vol. COM-29, pp. 1715-1720, Nov. 1981.
- [2] H. B. Poza, *et al.*, "A wideband data link computer simulation model," in *Proc. NAECON Conf.*, 1975.
- [3] M. T. Abuelma'atti, "Frequency-dependent nonlinear quadrature model for TWT amplifiers," *IEEE Trans. Comm.*, vol. COM-32, pp. 982-986, Aug. 1984.
- [4] R. G. Vaughan, *et al.*, "The theory of bandpass sampling," *IEEE Trans. Signal Processing*, vol. 39, no. 9, pp. 1973-1984, 1991.
- [5] G. Hill, "The benefits of undersampling," *Electron. Design*, pp. 69-79, July 11, 1994.
- [6] J. A. Wepman, "Analog-to-digital converters and their applications in radio receivers," *IEEE Commun. Mag.*, pp. 39-45, May 1995.
- [7] V. Borich, *et al.*, "Nonlinear effects of power amplification on multicarrier spread spectrum systems," in *IEEE MTT-S Dig.*, 1998, pp. 323-326.
- [8] M. S. Heutmaker, *et al.*, "Envelope distortion models with memory improve the prediction of spectral regrowth for some RF amplifiers," in *48th ARFTG Conf. Dig.*, 1996.
- [9] W. Greblicki, "Nonlinearity estimation in Hammerstein systems based on ordered observations," *IEEE Trans. Signal Processing*, vol. 44, pp. 1224-1233, May 1996.
- [10] M. Ibnkahla, *et al.*, "Neural network modeling and identification of nonlinear channels with memory: Algorithms, applications and analytic models," *IEEE Trans. Signal Processing*, vol. 46, pp. 1208-1220, May 1998.
- [11] M. S. Heutmaker, "The error vector and power amplifier distortion," *IEEE Wireless Comm. Conf.*, pp. 100-104, 1997.
- [12] C. J. Clark, *et al.*, "Time-domain envelope measurement technique with application to wideband power amplifier modeling," *IEEE Trans. Microwave Theory Tech.*, vol. 46, pp. 1531-1540, Dec. 1998.
- [13] J. Candy and G. Temes, "Oversampling methods for A/D and D/A conversion," in *Oversampling Delta-Sigma Data Converters*. New York: IEEE Press, 1992, pp. 1-25.
- [14] M. C. Jeruchim, P. Balaban, and K. S. Shanmugan, *Simulation of Communication Systems*. New York: Plenum, 1992.

Jesús Ibáñez-Díaz was born in Santander, Spain, in 1971. He received the Radiocommunication Bachelor Engineer degree and the Telecomm Engineer degree from the Universidad de Cantabria, Spain, in 1992 and 1995, respectively.

In 1995, he joined the Departamento de Ingeniería de Comunicaciones at the Universidad de Cantabria, Spain, where he is currently an Associate Professor. His research interest include digital signal processing, digital communication systems and nonlinear systems.

Carlos Pantaleón (M'95) was born in Badajoz, Spain, in 1966. He received the Telecommunication Engineer degree and the Doctor degree from the Universidad Politécnica de Madrid (UPM), Spain, in 1990 and 1994, respectively.

In 1990, he joined the Departamento de Ingeniería de Comunicaciones at the Universidad de Cantabria, Spain, where he is currently an Associate Professor. His research interests include digital signal processing, nonlinear systems and neural networks.

Ignacio Santamaría (A'96) was born in Vitoria, Spain, in 1967. He received the Telecommunication Engineer degree and the Doctor degree from the Universidad Politécnica de Madrid (UPM), Spain, in 1991 and 1995, respectively.

In 1992, he joined the Departamento de Ingeniería de Comunicaciones at the Universidad de Cantabria, Spain, where he is currently an Associate Professor. His research interests include digital signal processing, nonlinear systems and neural networks.

Tomás Fernández was born in Torrelavega, Spain, in 1966. He graduated in physics in 1991, and received the Doctor of physics degree in 1996, both from the University of Cantabria, Santander, Spain.

Since 1998, he has been Lecturer in the Department of Communications Engineering of the University of Cantabria. His past and present research interests include large-signal non linear modeling of III-V compounds transistors and Si-Ge HBT. Currently, his work is focused in the problematic of the behavior dependence of such us devices on thermal and frequency effects. He has participated in several researching projects (ESPRIT, TMR, etc.), as well as industrial RF & microwave projects with Spanish and European companies.

David Martínez was born in Santander, Spain in 1976. He graduated in telecommunication engineering in 1999 from the University of Cantabria, Santander, Spain.

In January of 2000, he engaged the Communication Engineering Department of the University of Cantabria, developing communication systems hardware for LMDS. Nowadays, he is working with ACORDE S.A. (a Spanish telecommunication research and development company) on highly linear power amplifiers and low-phase noise oscillators for microwave communication systems.